This is an *Accepted Manuscript*, which has been through the Royal Society of Chemistry peer review process and has been accepted for publication.

Accepted Manuscripts are published online shortly after acceptance, before technical editing, formatting and proof reading. Using this free service, authors can make their results available to the community, in citable form, before we publish the edited article. We will replace this *Accepted Manuscript* with the edited and formatted *Advance Article* as soon as it is available.

You can find more information about *Accepted Manuscripts* in the **Information for Authors**.

Journal Name

Dynamic Article Links ▶

ARTICLE TYPE

Dinuclear osmium(II) probes for high-resolution visualisation of cellular DNA structure using electron microscopy

Ashley Wragg,[a] Martin R. Gill,[b] Christopher J. Hill,[b] Xiaodi Su,[c] Anthony J. H. M. Meijer,[a] Carl Smythe,*[b] and Jim A. Thomas*[a]

Two dinuclear osmium polypyridyl complexes function as convenient, easy to handle TEM contrast agents and facilitate the high-resolution visualisation of intracellular structure,
10 **particularly sub-nuclear detail.**

The high-resolution technique transmission electron microscopy (TEM) is an indispensable tool for cell biology and medicine, providing vital information on cell structure and function. Micrographs are commonly stained with osmium tetroxide
15 (OsO_4) as this facilitates the visualisation of intracellular structure courtesy of its dense membrane staining.[1] However, despite its widespread use, OsO_4 is far from an idea reagent: it is a volatile, highly toxic complex. It possess a high vapour pressure and exposures as low as 0.1 mg/m^3 has been reported to cause short-
20 term effects such as tearing, vision disturbances ("hallucinations" of halos of light), headaches and conjunctivitis.[2] Given these factors, considerable care must be taken in handling OsO_4. Despite these concerns, syntheses of alternative osmium TEM stains are virtually unreported, with poor aqueous solubility
25 ascribed as the main factor impeding development.[3]

One class of compounds of recent biological interest are transition metal complexes that interact with DNA through non-covalent binding modes.[4] Although osmium(II) polypyridyl complexes can bind DNA though reversible mechanisms with
30 high affinity,[5, 6] because of their poor emission properties, they are considerably less studied than their ruthenium counterparts.[7, 8] This is surprising as such systems are ideal candidates for use with TEM, as they are kinetically unreactive and possess a highly electron-dense third row transition metal centre. Considering the
35 dearth of nucleic acid specific TEM stains,[9-13] the use of low-toxicity, easy-to-handle, Os^{II} polypyridyl complexes to image crucially important biomolecules through TEM is a very attractive goal.

Herein, we report on two dinuclear osmium tpphz complexes,
40 previously reported [(Os(bipy)$_2$)$_2$tpphz)]$^{4+}$ (**1**) and the new complex [(Os(phen)$_2$)$_2$tpphz)]$^{4+}$ (**2**) (bipy = bipy = 2,2'-bipyridine, phen = 1,10-phenanthroline,tpphz = (tetrapyrido[3,2-a:2',3'-c:3'',2''-h:2''',3'''-j]phenazine) – Scheme 1 - quantifying their thermal stability, their *in vitro* DNA binding and their ability
45 to visualise intracellular structure using electron microscopy.

Complexes **1** and **2** were prepared through adaptation of a reported methods.[14,15] Both complexes were fully characterised by ^{1}H NMR, CHN analysis, and mass spectrometry. UV-visible absorption spectra of the hexafluorophosphate and chloride salts
50 of **2** were recorded in freshly distilled dry acetonitrile and double distilled water respectively (see ESI†). The absorption spectrum of **1** is in agreement with previously reported data,[14] which facilitated the assignments for the spectrum of **2**. The strong absorption bands in the UV (< 350 nm) are assigned to LC
55 (ligand-centred) transitions (ε up to 10^6 M^{-1}). Two absorption bands at 360 nm are characteristic of tpphz-centred transitions.[6] Above 370 nm, broader lower energy absorptions of spin allowed ^{1}MLCT transition, with a low energy ^{3}MLCT shoulder are observed. In agreement with previous studies on **1**,[14] due to
60 energy gap law effects[16] neither of the complexes demonstrated significant luminescence at room temperature in acetonitrile.
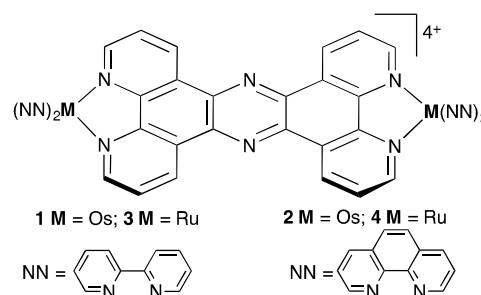
Scheme 1 – the structures of complexes discussed in this study

As outlined above, the high volatility of OsO_4 presents
65 significant challenges in its use as a reagent. To assess the comparative stability of **1** and **2**, thermal gravimetric analyses (TGA) were carried out. For further comparison these studies also included the analogous ruthenium complexes **3** and **4**. TGA experiments revealed that degradation of all four complexes only
70 occurs at high temperatures. A loss in weight for **1** is observed at 370 ^{o}C; whilst, even at 600 ^{o}C, **2** displayed almost no loss in weight (Fig 1). Losses in weight for **3** and **4** similar to those observed for **2** are observed at 325 ^{o}C and 250 ^{o}C respectively, with **3** completely decomposing at ~ 400 ^{o}C. These results
75 indicate that - as expected from their respective Os-N bond strengths - both osmium complexes show extremely low volatility and are considerably more stable than even their ruthenium analogues. It is also apparent that both phenanthroline complexes are more stable than their bipyridyl analogues; highlighting the
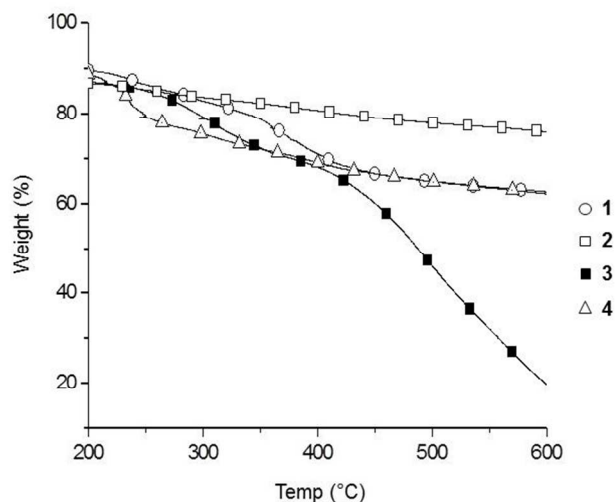80 effect of ancillary ligand in overall complex stability.

Fig 1. Thermal gravimetric analysis for **1 – 4**.

Previously reported studies have shown that, due to their close structural similarities, the biological interactions of inert Os[II]
[5] systems are identical to those of their Ru[II] analogues[17]. Certainly, comparisons between each of the Os[II] complexes and their Ru[II] analogues through DFT methods reveal that the structures and their electrostatic potential distributions are effectively identical (Fig. 2), illustrated by the fact that the Tanimoto similarity index
[10] for **2** and **4** is 0.999. Unsurprisingly, therefore, the effect of CT-DNA addition on the UV-Vis spectra of the complexes, in which considerable hypochromism of MLCT-bands is observed (see Fig. S1†) is consistent with the same high-affinity interaction observed for **3** and **4**.[18]
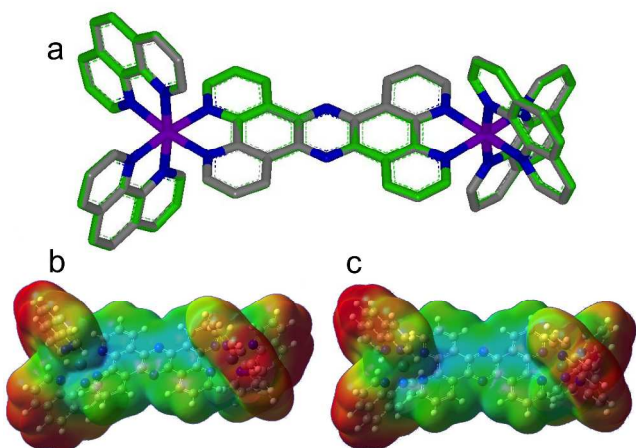

Fig 2. Results obtained from DFT calculations. (a) Overlay of calculated structures of **2** and **4**. (b, c) Electrostatic potential of **2** (b) and **4** (c).

Although TEM has previously been used to investigate localisation of cytotoxic Os-based therapeutics,[19] the aim of this
[20] study was to identify an effective TEM contrast reagent of low toxicity. Consequently, we first measured the cytotoxicity of **1** and **2** towards MCF-7 human breast cancer cells. For a 24 h exposure time to a concentration gradient of each complex, **1** showed negligible impact upon cell viability (half inhibitory
[25] concentration, IC_{50} > 200 uM) while **2** demonstrated activity only at 200 μM and possessed an IC_{50} value of 146 +/- 14 μM (Fig.

S2†). These values indicate that the cytotoxicities of **1** and **2** are significantly lower than those of Os(II) compounds containing labile ligands,[19] and are in close agreement with the
[30] corresponding figures for their ruthenium analogues.[20] Both these observations support the hypothesis that **1** and **2** contain unreactive osmium centres, and further confirms that the substitution of Ru[II] centres with Os[II] units has no effect on the biomolecular properties of these systems.
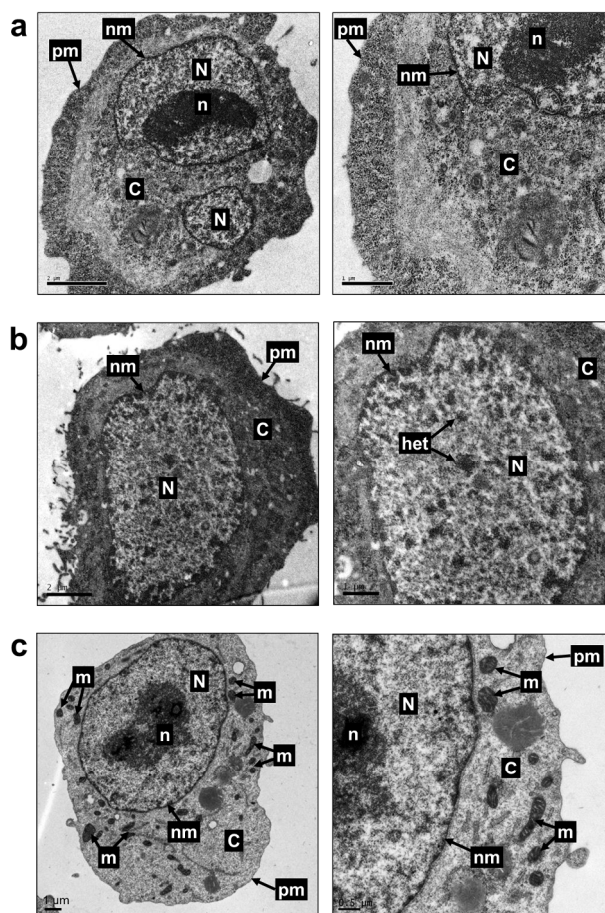

Fig 3 (a) Fixed A2780 cell stained with **1** and visualised by TEM. (b) TEM of fixed MCF7 cell stained with **2**. Higher magnification images shown on right hand panels. Key: pm = plasma membrane, nm = nuclear membrane, N = nucleus, C = cytosol, n = nucleolus, het = hetrochromatin
[40] (c) Fixed A2780 cell stained solely with OsO4 for reference

Given the advantageous low levels of cytotoxicity observed, the potential of each complex to function as TEM-based stains was investigated. This involved replacing toxic OsO_4 with aqueous solutions of **1** or **2** during standard TEM sample
[45] preparation for cells grown in culture. MCF7 (human breast cancer) or A2780 (human ovarian cancer) cells were fixed with glutaraldehyde, permeablised with 70% ethanol, and incubated with solutions of 500 μM **1** or 1 mM **2** overnight. Samples were embedded in Araldite® resin, ultrathin sections obtained and
[50] visualised using TEM. To obtain higher detail in cytological TEM images, researchers commonly stain sections with additional metal ions (e.g. uranyl acetate or lead citrate).[1] In this case however, no other stain was applied as this enabled the potential of each dinuclear Os(II) tpphz complex as TEM contrast

agents to be assessed and compared. Applying this methodology, cells stained with **1** or **2** display excellent levels of intracellular contrast, which facilities the visualisation of cellular detail at high resolution that is comparable to those obtained by OsO_4 (Figs 3 and S3†).

In particular, staining with either compound generates clear definition of the cell nucleus while nucleoli especially are densely stained in the case of **1** (Fig 3a). Higher magnification reveals a strong heterochromatin sub-nuclear staining pattern, where the nuclear membrane is also clearly defined (Fig 3a and 3b, right hand panels). Thus, **1** and **2** function as nuclear DNA stains for electron microscopy; results in agreement with their high reversible binding affinity. In addition to the clear nuclear definition observed, cells stained with either **1** or **2** additionally display unusual staining of the cytoplasm, where different contrast levels are clearly observed (particularly observable in Fig 3a). It seems that this "two toned" cytoplasmic staining is the result of a concentration gradient involving the stains, although the exact nature of this effect is unknown. Comparisons with cells imaged with OsO_4 (Fig 3c) show that whilst **1** and **2** provide similar levels of contrast, they do not target membrane based structures as clearly compared to the conventional osmium stain.

In addition to the staining of prepared samples after fixation, TEM may also be applied pre-fixation to assess the cellular uptake and localisation of cells incubated with metal-containing compounds. This approach is commonly employed for metal-based nanoparticles[21, 22] as well as the live cell distribution metal anticancer compounds.[19, 23, 24] In this latter case it has provided information on biomolecular targeting and mechanism of action of therapeutic leads, where a particularly relevant example identified the accumulation of an osmium anti-cancer complex within the nucleus and mitochondria of apoptotic cells.[19] With this in mind, live MCF7 cells were incubated with solutions of **1** or **2** before samples were processed for TEM as described above –Figure 4.
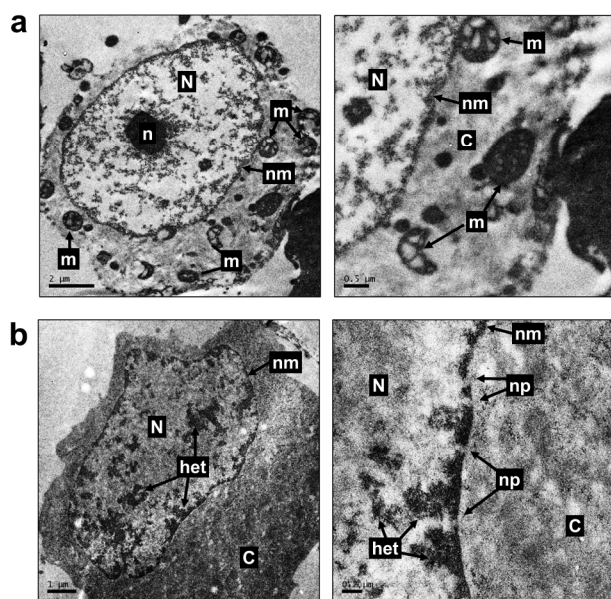
a

b

Fig 4 (a) TEM showing necrotic MCF7 cell visualised by **1** (500 µM, 1 h). Note preserved organelle structures (right). (b) Successful nuclear internalisation of **2** by MCF7 cell (500 µM, 1 h), as visualised by TEM.

Key: pm = plasma membrane, nm = nuclear membrane, N = nucleus, C = cytosol, n = nucleolus, m = mitochondria, het = hetrochromatin, np = nuclear pore complex

As for fixed cell staining, to aid assignments and comparisons no other contrast agent was employed during these studies. Applying these incubation conditions, the majority of cells exposed to **1** demonstrated poor intracellular definition (Fig S4†). However, cells undergoing necrosis are clearly defined by the strong contrast provided by **1**, an example of which is shown in Figure 4a. This cell shows strong staining of the inner nuclear membrane with the nucleoli being densely-stained in a similar manner as for fixed cells. Clear definition of mitochondrial structure is also evident (Fig. 4a – right hand image). As a cell in this late stage of necrosis will possess a perforated plasma membrane, this serves as a useful reference for the ability of **1** to stain intracellular organelles once the barrier of cell uptake has been broken. Classical necrosis is generally defined by cell swelling, the preservation of intracellular and ultimately the loss of plasma membrane integrity. While apoptosis or "programmed cell death" is a more studied cell death pathway, recent research has shown necrotic-type pathways can demonstrate similarly high levels of regulation.[25] In this context, **1** may use have uses in the isolation and study of the structural features during necrotic cell death. The strong nucleolar density in stained cells obtained by both preparation techniques in this work is of interest. The accumulation of **1** within this densely packed, RNA-containing structure would likely indicate the complex demonstrates an affinity for this nucleic acid. Indeed, RNA binding studies on inert metal complexes have often been neglected in favour of the more stable DNA structure.

In contrast to the results obtained for **1**, cells incubated with **2** and then processed for TEM result in clear contrast facilitating the visualisation of intracellular detail (Figs 4b and S5†). The superior contrast provided within cells incubated with **2** compared to **1** is most likely explained by the phenanthroline derivative **2** displaying a greater rate of cell uptake than the bipyridine complex **1**. This would be in agreement with results for the analogous ruthenium compounds **3** and **4**,[20] and is not surprising given the structural similarity between complexes of osmium(II) and ruthenium(II). Intracellular contrast provided by the internalisation of **2** is particularly apparent within the cell nucleus, indicating high levels of uptake of **2** into this organelle. Examining the sub-nuclear structure in more detail, heterochromatin is densely stained by the complex, indicating **2** is targeting these densely-packed regions of DNA (Figs 4b and S5†). In a striking result, at higher magnification it is apparent the nuclear staining by **2** facilitates the visualisation of nuclear pore complexes; structures ~120 nm in diameter that are responsible for transport of molecules across the nuclear membrane (Fig. 4b, right hand image). Along with the fixed cell staining results, this further emphasises the ability of **2** to function as a DNA imaging agent for TEM.

In conclusion, chemically stable, water-soluble and non-volatile osmium polypyridyl complexes **1** and **2** function as excellent contrast stains for TEM, facilitating visualisation of sub-nuclear structure. This indicates that inert easy-to-handle osmium polypyridyl complexes may have a role as versatile electron microscopy stains. Since previous studies have

demonstrated that intracellular targeting of the ruthenium(II) analogues of **1** and **2** can be modulated through simple changes in their basic molecular architectures,[26] it is likely that this strategy can similarly be extended to develop a range of structure-specific probes.

Notes and references

ᵃ Department of Chemistry, University of Sheffield, Sheffield, S3 7HF UK. E-mail: james.thomas@sheffield.ac.uk
ᵇ Department of Biomedical Science, University of Sheffield, Sheffield, S3 7HF UK. E-mail: c.g.w.smythe@sheffield.ac.uk
ᶜ Institute of Material Research and Engineering, A*STAR (Agency for Science, Technology and Research), 3 Research Link, Singapore 117602.

† Electronic Supplementary Information (ESI) available: syntheses, details of absoption soectra, DNA tirtations, cytotocity data, further TEM images See DOI: 10.1039/b000000x/

1. A. B. Maunsbach and B. A. Afzelius, *Biomedical Electron Microscopy: Illustrated Methods and Interpretations*, Academic Press, USA, 1999.
2. http://www.michigan.gov/documents/mdch-osmium_tetroxide_fs_109244_7.pdf
3. J. S. Hanker, D. K. Romanovicz and H. A. Padykula, *Histochemistry*, 1976, **49**, 263.
4. C. Metcalfe and J. A. Thomas, *Chem. Soc. Rev.*, 2003, **32**, 215.
5. R. E. Holmlin and J. K. Barton, *Inorg. Chem.*, 1995, **34**, 7.
6. R. E. Holmlin, E. D. A. Stemp and J. K. Barton, *J. Am. Chem. Soc.*, 1996, **118**, 5236.
7. A. E. Friedman, J. C. Chambron, J. P. Sauvage, N. J. Turro and J. K. Barton, *J. Am. Chem. Soc.*, 1990, **112**, 4960.
8. K. E. Erkkila, D. T. Odom and J. K. Barton, *Chem. Rev.*, 1999, **99**, 2777.
9. W. Bernhard and N. Granboulan, *Exp. Cell Res.*, 1963, **9**, 19.
10. P. Albersheim and U. Killias, *J. Cell Biol.*, 1963, **17**, 93.
11. S. K. Aggarwal, *J. Histochem. Cytochem.*, 1976, **24**, 984.
12. P. M. Charest, F. Bergeron and J. G. Lafontaine, *Histochem. J.*, 1985, **17**, 957.
13. M. Derenzini and F. Farabegoli, *J. Histochem. Cytochem.*, 1990, **38**, 1495.
14. J. Bolger, A. Gourdon, E. Ishow and J.-P. Launay, *Inorg. Chem.*, 1996, **35**, 2937.
15. P. Lay, A. M. Sargeson and H. Taube, in *Inorg. Synth.*, ed. J. M. Shreeve, John Wiley & Sons, Inc., Hoboken, NJ, USA, 1986, vol. 24, p. 295.
16. J. V. Caspar, E. M. Kober, B. P. Sullivan and T. J. Meyer, *J. Am. Chem. Soc.*, 1982, **104**, 630.
17. J. Maksimoska, D. S. Williams, G. E. Atilla-Gokcumen, K. S. M. Smalley, P. J. Carroll, R. D. Webster, P. Filippakopoulos, S. Knapp, M. Herlyn and E. Meggers, *Chem. Eur. J.*, 2008, **14**, 4816.
18. C. Rajput, R. Rutkaite, L. Swanson, I. Haq and J. A. Thomas, *Chem. Eur. J.*, 2006, **12**, 4611.
19. S. H. van Rijt, A. Mukherjee, A. M. Pizarro and P. J. Sadler, *J. Med. Chem.*, 2010, **53**, 840.
20. M. R. Gill, J. Garcia-Lara, S. J. Foster, C. Smythe, G. Battaglia and J. A. Thomas, *Nat. Chem.*, 2009, **1**, 662.
21. B. D. Chithrani, A. A. Ghazani and W. C. W. Chan, *Nano Lett.*, 2006, **6**, 662.
22. R. B. P. Elmes, K. N. Orange, S. M. Cloonan, D. C. Williams and T. Gunnlaugsson, *J. Am. Chem. Soc.*, 2011, **133**, 15862.
23. G. Sava, S. Zorzet, C. Turrin, F. Vita, M. Soranzo, G. Zabucchi, M. Cocchietto, A. Bergamo, S. DiGiovine, G. Pezzoni, L. Sartor and S. Garbisa, *Clin. Cancer Res.*, 2003, **9**, 1898.
24. A. Leonidova, V. Pierroz, R. Rubbiani, Y. Lan, A. G. Schmitz, A. Kaech, R. K. O. Sigel, S. Ferrari and G. Gasser, *Chem. Sci.*, 2014.
25. T. V. Berghe, N. Vanlangenakker, E. Parthoens, W. Deckers, M. Devos, N. Festjens, C. J. Guerin, U. T. Brunk, W. Declercq and P. Vandenabeele, *Cell Death Diff.*, 2010, **17**, 922.
26. M. R. Gill, D. Cecchin, M. G. Walker, R. S. Mulla, G. Battaglia, C. Smythe, and J. A. Thomas, *Chem. Sci.*, 2013, **4**, 512

ChemComm Accepted Manuscript